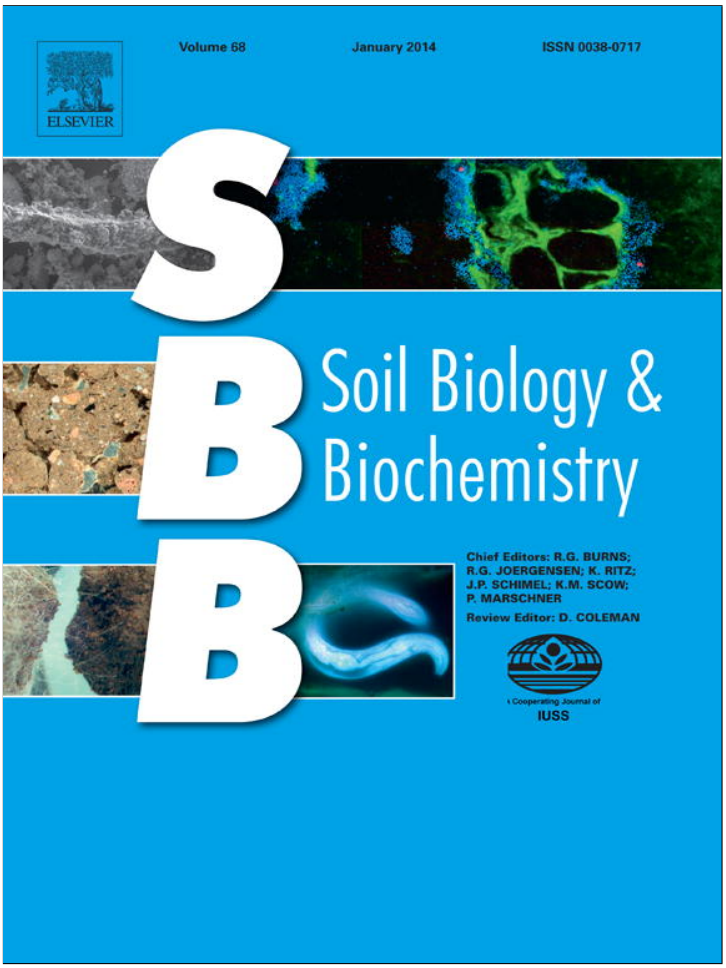

Soil Biology & Biochemistry 68 (2014) 329–336

Contents lists available at ScienceDirect

Soil Biology & Biochemistry

journal homepage: www.elsevier.com/locate/soilbio

Pulse-dynamic and monotonic decline patterns of soil respiration in long term laboratory microcosms

Qiuxiang Tian [a,b,1], Hongbo He [a,1], Weixin Cheng [a,c,1], Xudong Zhang [a,d,*,1]

[a] State Key Laboratory of Forest and Soil Ecology, Institute of Applied Ecology, Chinese Academy of Sciences, Shenyang 110164, China
[b] University of Chinese Academy of Sciences, Beijing 100049, China
[c] Environmental Studies Department, University of California, Santa Cruz, CA 95064, USA
[d] National Field Observation and Research Station of Shenyang Agro-Ecosystems, Shenyang 110016, China

ARTICLE INFO

Article history:
Received 31 May 2013
Received in revised form
9 September 2013
Accepted 10 October 2013
Available online 22 October 2013

Keywords:
Soil respiration
Pulse-dynamic
First-order kinetics
Soil carbon pool
Substrate availability
Soil texture
Static view

ABSTRACT

Carbon dioxide from soil respiration is a key source of atmospheric CO_2 and a major component of the global carbon cycle. However, the temporal pattern of soil respiration is not well understood and even wrongly modeled. In a 360-day laboratory experiment, we investigated temporal patterns of soil respiration and microbial carbon availability using five soils taken from five altitudinal zones on a temperate Mountain. We found two distinctive patterns in soil respiration and carbon availability among the five soils: a new pulse-dynamic pattern for soils taken from middle altitudinal zones, and the commonly reported pattern of monotonic decline for other soils. Our redundancy analysis further showed that soil texture plays a major role in determining the occurrence and magnitude of the pulse-dynamic pattern. The new pulse-dynamic pattern challenges the commonly held static view of soil organic carbon mineralization, and has crucial implications for modeling soil carbon in terrestrial ecosystems.

1. Introduction

Soil respiration is a main process determining the size of the soil organic carbon (SOC) pool, the largest terrestrial carbon reservoir; and annual soil CO_2 efflux from global soil respiration is approximately 9 times more than that from fossil fuel burning (Raich and Potter, 1995). Therefore, soil respiration plays critical roles in regulating atmospheric CO_2 concentrations and climate dynamics (Davidson and Janssens, 2006). Understanding soil respiration is crucial for predicting changes in the global carbon cycle in response to global environmental change. However, due to methodological or logistical constraints, the mechanisms and factors controlling soil respiration are still not fully understood.

Soil incubation experiments have been widely used to improve our understanding of soil respiration (von Lutzow and Kogel-Knabner, 2009) because they allow precise control of the environmental variables and comparisons of SOC mineralization rates of different soils under the same environmental conditions (Rey and Jarvis, 2006). As demonstrated by many laboratory incubation studies, soil respiration is strongly regulated by the quantity and the quality of soil organic matter as the general source of microbial substrates (Wang et al., 2003, 2004; Engelking et al., 2007; He et al., 2011; Gude et al., 2012). Soil organic matter consists of a large number of ill defined organic groups, of varying microbial availability, ranging from simple compounds to highly complex, stable structures with mean residence times ranging from days to thousands of years (van Hees et al., 2008). Because of the large heterogeneity of soil microbial substrates, understanding the relationship between substrate supply and respiratory CO_2 production during SOM decomposition has been extremely difficult (Olk, 2006). This difficulty has been dealt with in most ecosystem carbon models (e.g., Rothamsted model-RothC and CENTURY) by dividing, soil organic matter into different pools with specific decomposition rates according to first-order kinetic functions (Luo and Zhou, 2006). By using the first-order kinetic model approach, one assumes that each soil sample contains a number of organic pools each of which has a fixed quantity at the start of the experiment and a corresponding constant of decomposition rate; and consequently soil CO_2 evolution rate through time from soil

* Corresponding author. State Key Laboratory of Forest and Soil Ecology, Institute of Applied Ecology, Chinese Academy of Sciences, Shenyang 110164, China. Tel.: +86 024 83970375.
E-mail address: xdzhang@iae.ac.cn (X. Zhang).
[1] All four authors contributed equally.

0038-0717/$ – see front matter © 2013 Elsevier Ltd. All rights reserved.
http://dx.doi.org/10.1016/j.soilbio.2013.10.015

incubation experiments would follow a pattern of monotonic decline since the quantity of each pool will only become smaller as decomposition proceeds. This generally represents the fixed/static view of soil organic matter decomposition (Fig. 1), even though these pools have rarely been empirically defined and quantified.

This static view is empirically supported by the apparent good fit between cumulative CO_2 efflux rates through incubation time and the two- or three-pool first-order kinetic model (Collins et al., 1999; Knorr et al., 2005; Rey and Jarvis, 2006). Because of the apparent good fit, this approach has been widely used in analyzing empirical data of soil respiration for estimating SOC pool sizes and their corresponding mineralization constants (Knorr et al., 2005). However, this approach has two key issues. First, expressing SOC mineralization in the form of cumulative CO_2 efflux rates through incubation time obscures pulse dynamic patterns in real time soil respiration rates (Fig. 1). Second, other factors (e.g., soil structure) which may affect substrate availability are largely ignored.

This static view of SOC mineralization also stems from the hypothesis that the chemical nature of each pool is the sole determinant of its decomposition rate. However, recent evidence suggests that this hypothesis needs major revision (Schmidt et al., 2011). For example, some chemically labile substrates can be physically protected within soil aggregates and be inaccessible for microbial use (Sollins et al., 1996; Six et al., 2002). During the incubation, new soil aggregates may form and some existing aggregates may become unstable and separate, which may change both the physical protection and availability of SOC (Conant et al., 2011), and ultimately produce pulses of CO_2 during the incubation. Furthermore, virtually all studies of priming effects reveal pulses of CO_2 evolution from the decomposition of SOC after addition of labile substrates (Kuzyakov, 2010), clearly indicating that soil substrates are highly dynamic and should not be represented by fixed/static pools (Fig. 1). However, specific study focusing on such dynamic changes is still lacking.

In order to address the two issues mentioned above and to illuminate the pulse dynamic nature of soil respiration, we carried out a 360-day incubation experiment using five soils collected along an elevation gradient on Changbai Mountain in northeastern China. Soil respiration rates, substrate availability, and microbial biomass were estimated throughout the incubation period. Because of methodological difficulties, substrate availability has rarely been quantified in pervious studies. In our research, the carbon availability index (CAI), expressed as the ratio of basal respiration rate to substrate-induced respiration rate, was used to represent the substrate availability (Cheng et al., 1996; Gershenson et al., 2009).

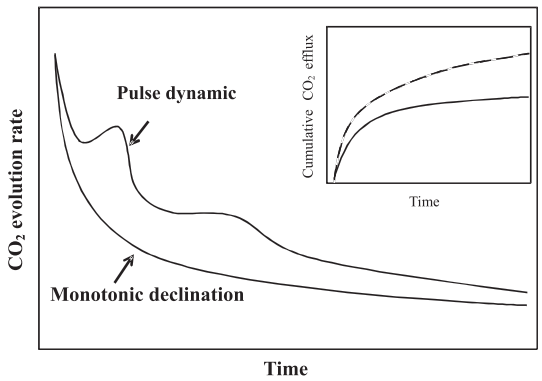

Fig. 1. Conceptual models of SOC decomposition: Commonly used models of fixed-pools with first-order kinetics predicts that soil CO_2 evolution rate from a soil incubation experiment with time would follow a pattern of monotonic decline; whereas a model based on information from studies of priming effect and other evidence would predicts that the CO_2 evolution rate would show a pattern of pulse-like fluctuations-or a pulse dynamic pattern. In the insert graph, the dashed line shows the cumulative CO_2 efflux with the pulse-dynamic pattern of soil respiration, and the solid line shows the cumulative CO_2 efflux with the monotonic decline pattern of soil respiration. Pulse dynamic patterns can be obscured if soil respiration is given as cumulative CO_2 efflux through time.

2. Materials and methods

2.1. Site description and soil sampling

The experimental sites were located in the Changbai Mountain National Nature Reserve (CMNNR) (41″ 58′–42″ 06′ N, 127″ 54′–128″ 08′ E), in Jilin Province of China with a total area of 196,465 ha. The sites have typical continental monsoon climates. With increasing altitude from 500 m to 2744 m above sea level, the mean annual temperature decreases from 3.5 to −7.4 °C, and the mean annual precipitation increases from 720 to 1400 mm. Precipitation occurs mainly from June to September, accounting for 60% of the annual precipitation. The distinct climate formed a clear vegetation gradient along the elevation gradient: *Pinus koraiensis* and broad-leaf mixed forest (500–1100 m), *Picea* and *Abies* forest (1100–1600 m), *Larix* and *Abies* forest (1600–1800 m), *Betula ermanii* forest (1800–2000 m), and alpine tundra (2000–2744 m). In this study, we sampled the soils from mineral soil layers (A − horizon) in the five altitudinal zones on the northern slope of Changbai Mountain in the summer of 2010. The detailed information of these forest plots is provided in Table 1. Within each altitudinal zone, we collected soils from four randomly chosen locations. Visible roots and stone were removed by handpicking and an electrostatic method during sieving. Briefly, the soil samples were spread out on a paper. A polyethylene plate (length 400 mm and width 200 mm) was charged by means of intensive rubbing (3–4 s) on a stretched wool fabric. The plate was set over the padding with spread-out soil and the padding was shaken horizontally. By doing so, the roots were attracted by the charged plate and collected manually. All field samples were homogenized, air-dried, and stored at room temperature (20 °C) for incubation.

2.2. Laboratory incubation

For each of the five soils along the elevation gradient, 60 laboratory replicate samples (25 g dry soil per sample) were weighed and placed in plastic specimen bottles (150 mL, 3 cm diameter). Before starting the experimental incubation, soil moisture was adjusted to 65% water-holding capacity (WHC) by adding deionized H_2O. WHC was determined by saturating a sample of soil in a filter paper placed in a glass funnel, and then permitting the water to drain for 2 h before determining the gravimetric soil moisture content (for 100% WHC) by drying for 24 h at 105 °C. Distilled water was added at regular intervals (4 days) to maintain the water content in the samples. All soil samples were incubated at 25 °C in an automatically controlled incubator for a total of 360 days. The accuracy of the temperature control of the incubator was ±0.05 °C.

2.3. Soil respiration measurements

Soil respiration was measured daily during the first week, weekly in the following three weeks, and monthly in the remaining period of the experiment. At each measurement time, three of the replicate samples were randomly chosen. Soil respiration was measured using the method described by Gershenson et al. (2009). Briefly, a 25 °C water bath was set up to keep temperature constant during the measurements. An air pump forced ambient air through a soda-lime column, thereby producing CO_2-free air. The CO_2-free

Table 1
Main characteristics of soil samples taken from five locations along the elevation gradient in the Changbai Mountain Reserve.

Site name	A	B	C	D	E
Elevation (m)	791	1247	1707	1975	2294
Mean temperature of growing season (°C)	15.75	13.38	12.29	11.52	9.95
Soil type	Albi-Boric Argosols	Bori-Udic Cambosols	Umbri-Gelic Cambosols	Permi-Gelic Cambosols	Udic-Andisols
Forest type	*Pinus koraiensis* and broadleaf mixed forest	*Picea* and *Abies* forest	*Larix* and *Abies* forest	*Betula ermanii* forest	Alpine tundra
Dominant plants	*Pinus koraiensis*, *Acer mono*, *Tilia amurensis*, *Ulmus mongolica*	*Picea koraiensis*, *P. koyamai* var. *koraiensis*, *Abies nephrolepis*	*Larix olgensis*, *Abies nephrolepis*, *Picea asperata*,	*Betula ermanii*, *Rhododendron chrysanthum*, *Juniperus sibirica*, *Veronica sibirica*	*Rhododendron chrysanthum*, *Dryas octopetala*, *Phyllodoce caerulea*, *Vaccinium vitis-idaea*
Soil organic C (mg g^{-1})	122.1 ± 4.10 d	78.2 ± 1.40 b	66.3 ± 0.76 a	113.4 ± 3.16 c	137.7 ± 3.61 e
Soil total N (mg g^{-1})	8.68 ± 0.22 e	3.77 ± 0.16 a	5.05 ± 0.06 b	5.67 ± 0.15 c	6.31 ± 0.37 d
C/N	14.1 ± 0.2 a	20.8 ± 1.3 b	13.1 ± 0.1 a	20.0 ± 0.1 b	21.9 ± 1.6 b
Light fraction carbon/TC (%)	2.00 ± 0.20 b	2.53 ± 0.38 b	1.22 ± 0.28 a	1.23 ± 0.06 a	2.33 ± 0.19 b
pH (1:2.5 soil:water)	6.24 ± 0.12 b	4.64 ± 0.07 a	4.61 ± 0.01 a	4.23 ± 0.12 a	4.54 ± 0.25 a
Soil available N (μg g^{-1})	540.4 ± 22.8 d	273.0 ± 10.9 a	421.4 ± 10.9 b	407.4 ± 16.8 b	490.7 ± 3.4 c
Soil available P (μg g^{-1})	13.57 ± 2.02 b	14.76 ± 0.82 b	11.43 ± 3.03 ab	8.81 ± 0.41 a	11.67 ± 1.65 ab
Soil available K (μg g^{-1})	281.9 ± 16.6 c	293.7 ± 16.6 c	199.7 ± 4.2 a	240.8 ± 8.3 b	293.7 ± 4.2 c
Sand% (2–0.05 mm)	15.13	39.75	27.14	37.37	47.15
Silt% (0.05–0.002 mm)	63.31	45.14	53.32	47.54	40.57
Clay% (<0.002 mm)	21.56	15.11	19.54	15.09	12.28

air then traveled through a copper coil submerged in the water bath, in order to equilibrate the air temperature with the temperature of the water bath. The CO_2-free air then entered a manifold, from which individual tubing led to the air inlet for each flask which contains a soil sample. The flow of air to each sample was controlled by a needle valve in order to ensure a constant flow rate (the average flow rate for all samples was 60 mL min^{-1}). After the flasks containing soil samples were put into the water baths, they were connected to the CO_2-free air manifold in order to ensure a supply of fresh air for the sample. One of the outlets was used as a blank reference without any soil sample. The flasks were allowed to adjust to the water bath temperature for 1 h. After 1 h, the outflow tubing of each sample was connected in turn to the flow meter and Li-COR 6262 Infrared Gas Analyzer (IRGA) (Li-COR Biosciences, Lincoln, NB, USA), and then the flow rate and CO_2 concentration were recorded. Respiration measurements on each sample lasted approximately 3 min.

2.4. Substrate-induced respiration

To estimate microbial biomass during the incubation, a substrate-induced respiration technique was used. After measuring basal respiration, glucose solution (60 g L^{-1}) was added to each sample using a 5 mL syringe with a needle tip, and then the respiration was measured again at 25 °C using the same procedure as above. SIR was assayed within 2 h after the glucose addition when respiration remained nearly constant during the initial 4 h period before any microbial growth was noted (Lin and Brookes, 1999). In this study, 6–10 mg glucose g^{-1} soil (depending on SOC) was used for soils, which ensure excess carbon for the use by microorganisms. Care was exercised to ensure even distribution of glucose without saturating the soil with liquid, which would restrict CO_2 evolution from the sample.

2.5. Soil properties

Soil organic carbon was determined by combustion with an elemental analyzer (Model CN, Elementar Analysen Systeme GmbH, Germany). Soil pH values were measured with a calomel electrode on a paste of 1:2.5 (w:v) of air dry soil and de-ionized water. Soil available nitrogen was determined using an alkaline hydrolysis method. Soil available phosphorous was extracted with 0.03 mol/L NH_4F, and detecting the absorbance on a spectrophotometer at 700 nm. Soil available potassium was extracted with 1.0 mol/L ammonium acetate (NH_4OAc), and measured by using emission flame spectrometry. The light fractionation of soil carbon was separated from the remainder using sodium polytungstate solution (von Lutzow et al., 2007), with a density of 1.6 g cm^{-3}. Soil texture was determined using a Bouyoucos hydrometer.

2.6. Calculation and statistics

The respiration rate of each soil sample was calculated from Gershenson et al. (2009):

$$R_r = 0.536 \times \left(C_c \times R_f\right) \Big/ W_s \quad (1)$$

where R_r is soil respiration (μg C g^{-1} soil h^{-1}), C_c is the recorded CO_2 concentration in μmol CO_2 mol^{-1}, R_f is the recorded flow rate in mL h^{-1}, and W_s was gram dry weight of the sample.

Microbial biomass carbon was calculated using substrate induced respiration according to Anderson and Domsch (1978) and adjusted to account for use at 25 °C (West and Sparling, 1986):

$$\mathrm{MB} = 32.8 \times R_{\mathrm{Gl}+} + 3.7 \quad (2)$$

where MB is microbial biomass carbon (μg C g^{-1} soil), R_{Gl+} the soil substrate induced respiration rate at 25 °C (μL CO_2 g^{-1} soil h^{-1}).

Carbon availability index was calculated by dividing the basal respiration rate with substrate-induced respiration rate from the same soil sample (Gershenson et al., 2009):

$$\mathrm{CAI} = R_{\mathrm{Gl}-}/R_{\mathrm{Gl}+} \quad (3)$$

where R_{Gl-} and R_{Gl+} are the basal respiration for ambient substrate and substrate-induced respiration, respectively. Because the substrate-induced respiration represents the maximum microbial respiration rate for each sample once the carbon limitation has been alleviated by adding adequate level of glucose (a commonly known “universal” carbon substrate), the ratio of the basal rate to the SIR indicates the relative carbon availability.

For all incubation samples, the soil respiration rate was expressed as μg CO_2–C g^{-1} soil carbon at the corresponding incubation time. The statistical differences in soil respiration rates, microbial biomass and CAI values among soils during the incubation were analyzed using one-way analysis of variance (ANOVA) with Tukey's honestly significant difference (HSD) as post hoc. Redundancy analysis (RDA) was performed to explore the relationship between soil respiration data (highly dynamic data from day-14 to day-140) and soil properties using software package Canoco 4.5 for Windows. A Monte Carlo test (499 permutations) based on the RDA was used to assess which variables had a significant influence on the dynamics of soil respiration. Correlation analysis among soil characteristics was carried out to remove some significantly correlated variables before RDA analysis. ANOVA and correlation analysis was performed using SPSS 13.0. Differences were considered statistically significant when $p < 0.05$.

3. Results

3.1. Soil properties at the altitude gradient

The physical and chemical properties of the investigated soils were given in Table 1. With the increase of elevation, the SOC contents declined from soil A to soil C, but then increased from soil C to soil E. Soil total nitrogen contents (TN) increased significantly from soil B to soil E, but the highest value was found in soil A. The C:N ratio for soil A and C was significantly lower than soil B, D and E. The light carbon fraction ranged from 12.2% (soil C) to 25.3% of total SOC. The content of soil available nutrients N, P and K did not show any altitudinal tendency among the five soils. Soil pH values ranged from 4.23 to 6.24. The textures of the five soils can be separated into two groups. Soils A and C were silty, while soils B, D and E were much sandy.

3.2. Temporal dynamics of soil respiration

The respiration rates of the five soils during the incubation time showed two distinct patterns (Fig. 2a). For soil B, D and E, respiration rates were highly dynamic. The respiration rate of soil B and D declined during the initial 30 days, and then surprisingly increased to a peak value from 30 to 70 days. The net increase for soil B from day-30 (the trough) to day-70 (the peak) was 30.19 μg CO_2–C g^{-1} soil carbon h^{-1}, which was 75 times larger than the overall standard error. For soil D, the net increase was 13.85 μg CO_2–C g^{-1} soil carbon h^{-1}, and 20 times the overall standard error. For soil E, the respiration was also dynamic, but the peak value occurred earlier (from 15 to 51 days) than the previous two. The net increase was 28 times the overall standard error. The respiration rates of these three soils showed pulse dynamic patterns, but those of soil A and C monotonically declined over the entire incubation period. The respiration rates of soil A declined sharply during the initial 30 days of incubation from 55.93 to 16.26 μg CO_2–C g^{-1} soil carbon h^{-1} and then decreased slowly from 16.26 to 5.24 μg CO_2–C g^{-1} soil carbon h^{-1} during the latter 330 days. The respiration rates of soil C declined sharply from 52.38 to 27.66 μg CO_2–C g^{-1} soil carbon h^{-1} during the initial 30 days of incubation and then decreased much slowly from 27.66 to 7.15 μg CO_2–C g^{-1} soil carbon h^{-1} during the latter 330 days. The respiration rates of these two soils during the incubation showed a pattern that has been commonly believed to be true for most soils.

In our analysis, all respiration rates were expressed as the rates of CO_2 release per unit of SOC. Therefore, the effect of different SOC contents on respiration rates was effectively removed, and the effect of decreasing SOC content during the incubation was also accounted for. The respiration rates of the five soils were

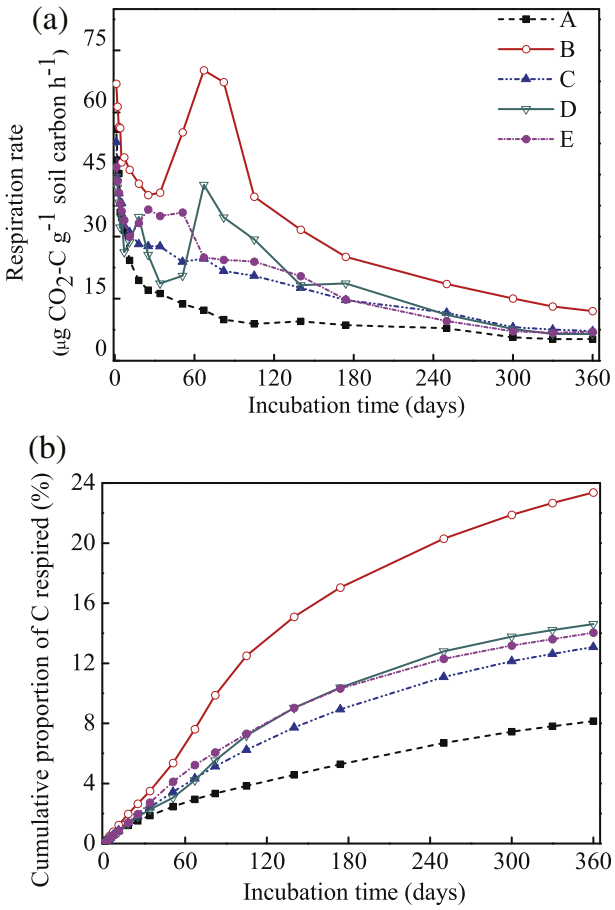

Fig. 2. Respiration rates (a) (μg CO_2–C g^{-1} soil carbon h^{-1}) and cumulative respired carbon (b) of soil samples from different elevations (A, B, C, D, and E) through incubation time. Each point in the plot represents the mean of 3 replicates ($n = 3$). The overall ANOVA standard error for soils A, B, C, D and E is 0.161, 0.400, 0.263, 0.699 and 0.206, respectively. A, B, C, D and E represents soils taken from *Pinus koraiensis* and broadleaf mixed forest, *Picea* and *Abies* forest, *Larix* and *Abies* forest, *Betula ermanii* forest, and alpine tundra, respectively.

significantly different from each other. The averaged respiration rate for the five soils over the entire experimental period was largest for soil B followed by D, E, and C, and the lowest for soil A. At the end of the incubation, the rate differences among the five soils narrowed down significantly.

The cumulative proportion of C respired leveled off with increasing incubation time (Fig. 2b). Over the entire incubation period, 8.15–23.36% of the initial soil C was decomposed with the order: B > D > E > C > A.

3.3. The changes of carbon availability during the incubation

Similar to the respiration rates during the incubation, carbon availability (Gershenson et al., 2009) also showed two distinct patterns (Fig. 3). For soil B, D and E, CAIs were highly dynamic. The CAI value of soil B and D declined during the initial 30 days of incubation and then sharply increased to a peak value of 0.476 from day 30 to 70, but increased again after day180 till the end. The net increase for soil B from day 30 (the trough) to day-70 (the peak) was 0.238, which was 79 times the overall standard error. The net increase for soil D was 0.238, 33 times the overall standard error. The CAI value of soil E peaked from day 10 to 50, earlier than soil B and D. The net increase was 47 times the overall standard error. For soil C, CAI value was dynamic, but showed somewhat a different

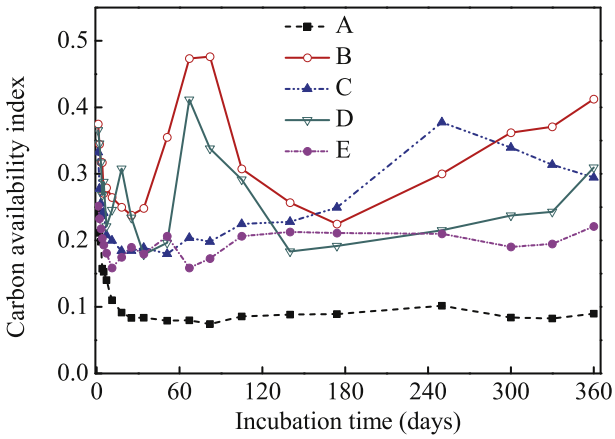

Fig. 3. The dynamics of carbon availability index (CAI) through incubation time The overall ANOVA standard error for soils A, B, C, D and E is 0.001, 0.003, 0.002, 0.007 and 0.001, respectively. The basal respiration rate divided by the substrate induced respiration rate of each soil sample was defined as carbon availability index.

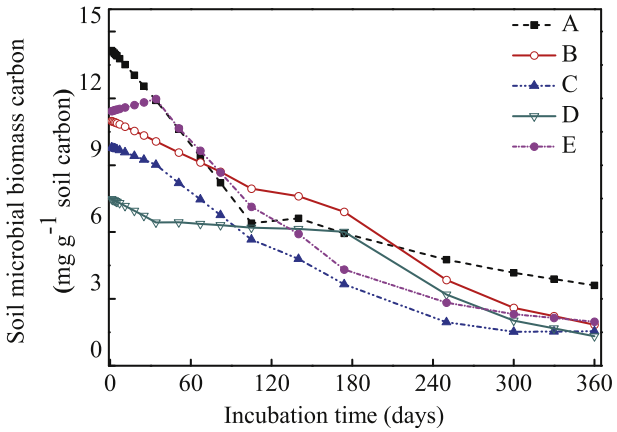

Fig. 4. The dynamics of soil microbial biomass carbon (mg g^{-1} soil carbon) through incubation time. The overall ANOVA standard error for soils A, B, C, D and E is 0.068, 0.231, 0.077, 0.048 and 0.059, respectively.

pattern than soil B, D or E, declined from 0.366 to 0.179 during the initial 30 days of incubation and then steadily increased to a peak value of 0.378 at day-250, declined again after day-250 till the end of the experiment. The net increase from day-30 (the trough) to day-250 (the peak) was 0.199, which was 99 times of the overall standard error. The CAI values of these four soils during the incubation all showed pulse dynamic patterns, instead of the commonly accepted simple pattern as was the case for soil A. The CAI value of soil A during the incubation period showed a "typical" pattern over the entire incubation period. It declined sharply during the initial 30 days from 0.243 to 0.084 and then remained constant (0.085 ± 0.007) for the latter 330 days.

The averaged CAI values of the five soils over the entire experimental period were significantly different from each other. The mean CAI value was largest for soil B followed by C, D, and E, and the lowest for soil A. This ordering sequence was in accordance with that of soil respiration.

3.4. The dynamics of soil microbial biomass carbon

We expressed the soil microbial biomass carbon values per unit of total soil carbon for the five soils, so that we could compare and contrast the biomass measurements through incubation time and across these soils with very different SOC contents, because the major effect of SOC content on biomass carbon was leveled by this expression. The microbial biomass of all five soils substantially declined during the experiment to 15.8–25% of the initial values (Fig. 4). Given this overall decline, there were some specific noteworthy phenomena. First, the microbial biomass values of the five soils were far apart at the beginning of the experiment, ranging from 7.48 to 14.15 mg g^{-1} soil carbon with an ascending ranking order of $D < C < B < E < A$. But the values for soils B, C, D and E converged to a narrow range of 1.32–1.98 mg g^{-1} soil carbon at the end of the experiment, except for soil A which had a significantly higher value than the other four soils at the end. Second, the microbial biomass carbon of soil E did not decline during the initial 30 days of the experiment, instead it increased to some degree, which differed from the rest of the soils. Third, the microbial biomass for soil D remained nearly constant from day-40 to day-180; and the microbial biomass for soil B showed the lowest rate of declination during the first half of the experimental period, even though the respiration rates and the CAIs for these two soils fluctuated to a large degree during this period.

3.5. Effects of soil properties on the pattern of soil respiration

The RDA results indicated that there were distinct differences in the dynamics of soil respiration between the five soil samples (Fig. 5). The first and second canonical axes explained 52.9% and 18.2% of the total variance of soil respiration data respectively. The dynamics of soil respiration in soils A and C were clearly different from those in soils B, D and E. The Monte Carlo test showed that the seven soil properties together explained 81% of the total variance of soil respiration data, but the content of sand particle alone explained 51% of the variance.

4. Discussion

Our results showed an unexpected new pulse-dynamic pattern of soil respiration during the incubation, which was in direct contrast to the commonly reported pattern of continued curve-linear decline. However, virtually all results from previous incubation experiments fit the continued curve-linear decline pattern in which soil respiration rates typically decline quickly at the

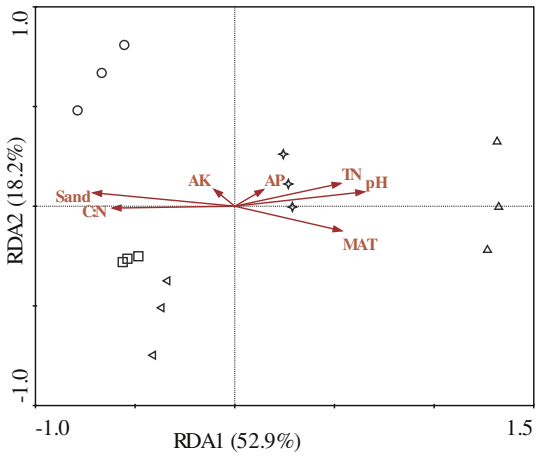

Fig. 5. Redundancy analysis (RDA) of soil respiration data and seven environment variables. Up-triangle, square, star, left-triangle and circle represents the soil taken from *Pinus koraiensis* and broadleaf mixed forest, *Picea* and *Abies* forest, *Larix* and *Abies* forest, *Betula ermanii* forest, and alpine tundra, respectively. Environmental variables are scaled by the solid axes. TN: total nitrogen; MAT: mean annual air temperature; AP: soil available phosphorous; AK: soil available potassium.

beginning of the incubation and then slowly as incubation goes longer. Although increases in soil respiration rates in the middle of incubations occurred in previous studies, they were often interpreted as procedural errors (Rey et al., 2008; Karhu et al., 2010; Plante et al., 2010; Xu et al., 2010; Haddix et al., 2011). This interpretation might be due to the use of alkaline absorption methods, which have much lower sensitivity and higher measurement errors than the method using infrared CO_2 analyzer, were often used in these studies. Another possible reason is that soil respiration is often expressed as cumulative CO_2 evolution, which tends to obscure pulses of soil respiration. Because we used an infrared CO_2 analyzer and expressed soil respiration at a much higher temporal resolution, the pulse-dynamic patterns for soils B, D and E in particular were abundantly clear because all the major pulses were measured as multiple points which were overwhelmingly higher than the corresponding statistical errors. Furthermore, this new pattern in soil respiration was also supported by our data set of CAI. The pulsing pattern in CAI offers a mechanistic support for the new pulse-dynamic pattern in soil respiration, as the pulsing changes in CAI were the primary drivers of the pulses in soil respiration. Both pulse patterns of soil respiration and CAI provide strong evidence supporting the dynamic pattern of SOC decomposition but opposing the static pattern as outlined in the introduction.

It is puzzling why the dynamic patterns occurred only in some soils, but not others. In addition, the duration and magnitude were also different between soil types. The results from the RDA analysis indicated that soil texture was the most important factor in determining the pattern of soil respiration. Soils showing the pulse-dynamic pattern (soils B, D and E) tended to have lower clay content and higher sand and silt contents. Substrates in small size particles could be more strongly protected than that in the larger ones and became inaccessible for microbial utilization (Verberne et al., 1990; von Lutzow et al., 2006; Traore et al., 2007). Therefore, substrate is more labile in sand fractions than in finer fractions. Wang et al. (2003) suggested that the protective effect of clay on SOC decomposition became significant as the substrate supply and microbial demand approached an equilibrium. Results from a study using a range of temperate conifer forest soils also indicated an interactive control of soil mineralogy and temperature on the availability of soil carbon pools or substrates to microbial mineralization (Rasmussen et al., 2006). Changes in soil aggregation is also suggested as a possible mechanism causing dynamic patterns because physical protection of organic matter within soil aggregates against microbial utilization is a key factor for soil organic matter stabilization (Sollins et al., 1996; Six et al., 2002). In principle, the de-aggregation effect in sandy soils (especially B and D) along the depletion of SOC during incubation should be stronger than in clay ones, but unfortunately we did not have data supporting this. Nevertheless, physical protection of SOC from microbial utilization by soil particles may play a major role in determining the level and occurrence of the pulse-dynamic patterns. In addition, vegetation did not contribute significantly to the pulse dynamic pattern. For instance, sites B and C are quite similar in terms of tree species, but both soil respiration and CAI patterns were markedly different. Sites B and E are totally different in terms of tree species, but both showed pulse dynamic patterns.

Another hypothesis is that changing soil microbial communities during the incubation caused the different patterns of soil respiration and CAI among these five soils. Shifts in microbial community structure were detected in previous laboratory incubation experiments (Zogg et al., 1997; Li et al., 2012). Another incubation experiment with soil of drained grassland also showed that incubation alone, regardless of environmental conditions, influenced bacterial communities (Stres et al., 2008). Generally accompanied with the change in microbial community structures, the amount and the kinds of extracellular enzymes would change simultaneously, which could alter the substrate availability to microbial mineralization (Schimel and Weintraub, 2003). The uncoupled nature between the generally decreasing trend of microbial biomass (Fig. 4) and the pulse-dynamic changes of CAI along the incubation (Fig. 3) indirectly suggests that substantial changes in the metabolic capabilities of soil microbial communities might occur during the incubation. Furthermore, CAIs for some soils (e.g., from sites B and D) in our experiment significantly increased during the later part of the incubation (Fig. 3) when the microbial biomass declined to very low levels (Fig. 4), indicating that the microbial communities near the end of the incubation were drastically different in metabolisms from the microbes at the early incubation time for soils B and D (note that these two soils showed the most pulsing dynamics). These preliminary results suggest that changing microbial community structure and activities could be a potential cause for the contrasting patterns in soil respiration and CAI. Undoubtedly, more studies are needed to further test this hypothesis.

The finding of the pulse-dynamic pattern of soil respiration directly challenges the static view of SOC decomposability because not all soils produced the monotonic decline pattern in soil respiration rates through time. This dynamic view of SOC mineralization is also indirectly supported by previous results. A recent report by Gauthier et al. (2010) showed that some soil carbon substrates might be released as pulses during soil microbial decomposition because the $\delta^{13}C$ value of respired CO_2 abruptly increased after 42 days of incubation for soils from a native oak-beech forest and a Douglas fir plantation. Similar changes in $\delta^{13}C$ values for a grassland soil were also reported by Pendall and King (2007). These sudden shifts of $\delta^{13}C$ were most likely from new carbon sources with different properties. Warming experiments also provided some indirect evidences for a dynamic change of substrate availability. For example, some SOC decomposition studies suggested that warming increased the fraction of soil carbon assimilated by microbes (Macdonald et al., 1995; Couteaux et al., 2002; Waldrop and Firestone, 2004; Larionova et al., 2007). An incubation experiment with intact soil cores of a frost-boil tundra ecosystem showed that the $\delta^{13}C$ values of CO_2 respired were negatively correlated with temperature, indicating the utilization of SOC fractions that were depleted in ^{13}C at higher temperatures (Biasi et al., 2005). Another incubation study with soils from free-air CO_2 enrichment (FACE) experiments also found that warming increased the mean age of respired carbon, which was showed by an immediate shift in the $\Delta^{14}C$ signature of respired CO_2 from warmed soils relative to the control soils (Hopkins et al., 2012). These published results indirectly suggest that both carbon pools and their availability have the potential to change in a dynamic way in response to changes in environmental conditions.

The finding of a pulse-dynamic pattern in soil respiration and carbon availability is also important because many current soil carbon models (e.g., Rothamsted model-RothC, CENTURY model, Terrestrial Ecosystem Model-TEM, PnEt-II, Linkages, Forest-BGC and Biome-BGC) are based on the static view which derives the decay constant of SOC by fitting a first-order kinetic function (Parton et al., 1987; Paustian et al., 1992; Collins et al., 1999; Knorr et al., 2005; Luo and Zhou, 2006) to cumulative soil CO_2 efflux rates from soil incubations. The mis-match in SOC mineralization patterns for some soils may have contributed to the high level of uncertainty in the terrestrial part of the global carbon cycle models (Heimann and Reichstein, 2008). Clearly, understanding the exact mechanisms causing these pulse-dynamic patterns warrants future research.

5. Conclusions

Our results showed a new pulse-dynamic pattern in both respiration and carbon availability for some soils during the incubation, while the "old" pattern of monotonic declination in soil respiration and carbon availability was found for some other soils. We hypothesized that the distinctive patterns between the two group of soils may stem from two potential mechanisms: (1) different soils possess different potentials in their physical protection of soil organic matter from microbial utilization by clay minerals and aggregation; and (2) the degree of changes in soil biological structure among the five soils during the incubation affects the patterns of soil respiration and carbon availability. The newly found pulse-dynamic pattern challenges the static view of soil organic matter decomposition, and has important implications for modeling of soil carbon in terrestrial ecosystems.

Acknowledgments

This research was jointly funded by the Natural Science Foundation of China, the National Key Basic Research Program of China and the International Partnership Program of Chinese Academy of Sciences. We thank Prof. Phillip Brookes at Rothamsted Experimental Station, UK for his advice and language revision.

References

Anderson, J.P.E., Domsch, K.H., 1978. Physiological method for quantitative measurement of microbial biomass in soils. Soil Biol. Biochem. 10, 215–221.
Biasi, C., Rusalimova, O., Meyer, H., Kaiser, C., Wanek, W., Barsukov, P., Junger, H., Richter, A., 2005. Temperature-dependent shift from labile to recalcitrant carbon sources of arctic heterotrophs. Rapid Commun. Mass Spectrom. 19, 1401–1408.
Cheng, W.X., Zhang, Q.L., Coleman, D.C., Carroll, C.R., Hoffman, C.A., 1996. Is available carbon limiting microbial respiration in the rhizosphere? Soil Biol. Biochem. 28, 1283–1288.
Collins, H.P., Blevins, R.L., Bundy, L.G., Christenson, D.R., Dick, W.A., Huggins, D.R., Paul, E.A., 1999. Soil carbon dynamics in corn-based agroecosystems: results from carbon-13 natural abundance. Soil Sci. Soc. Am. J. 63, 584–591.
Conant, R.T., Ryan, M.G., Agren, G.I., Birge, H.E., Davidson, E.A., Eliasson, P.E., Evans, S.E., Frey, S.D., Giardina, C.P., Hopkins, F.M., Hyvonen, R., Kirschbaum, M.U.F., Lavallee, J.M., Leifeld, J., Parton, W.J., Steinweg, J.M., Wallenstein, M.D., Wetterstedt, J.A.M., Bradford, M.A., 2011. Temperature and soil organic matter decomposition rates – synthesis of current knowledge and a way forward. Glob. Change Biol. 17, 3392–3404.
Couteaux, M.M., Sarmiento, L., Bottner, P., Acevedo, D., Thiery, J.M., 2002. Decomposition of standard plant material along an altitudinal transect (65–3968 m) in the tropical Andes. Soil Biol. Biochem. 34, 69–78.
Davidson, E.A., Janssens, I.A., 2006. Temperature sensitivity of soil carbon decomposition and feedbacks to climate change. Nature 440, 165–173.
Engelking, B., Flessa, H., Joergensen, R.G., 2007. Shifts in amino sugar and ergosterol contents after addition of sucrose and cellulose to soil. Soil Biol. Biochem. 39, 2111–2118.
Gauthier, A., Amiotte-Suchet, P., Nelson, P.N., Leveque, J., Zeller, B., Henault, C., 2010. Dynamics of the water extractable organic carbon pool during mineralisation in soils from a Douglas fir plantation and an oak-beech forest-an incubation experiment. Plant Soil 330, 465–479.
Gershenson, A., Bader, N.E., Cheng, W.X., 2009. Effects of substrate availability on the temperature sensitivity of soil organic matter decomposition. Glob. Change Biol. 15, 176–183.
Gude, A., Kandeler, E., Gleixner, G., 2012. Input related microbial carbon dynamic of soil organic matter in particle size fractions. Soil Biol. Biochem. 47, 209–219.
Haddix, M.L., Plante, A.F., Conant, R.T., Six, J., Steinweg, J.M., Magrini-Bair, K., Drijber, R.A., Morris, S.J., Paul, E.A., 2011. The role of soil characteristics on temperature sensitivity of soil organic matter. Soil Sci. Soc. Am. J. 75, 56–68.
He, H.B., Li, X.B., Zhang, W., Zhang, X.D., 2011. Differentiating the dynamics of native and newly immobilized amino sugars in soil frequently amended with inorganic nitrogen and glucose. Eur. J. Soil Sci. 62, 144–151.
Heimann, M., Reichstein, M., 2008. Terrestrial ecosystem carbon dynamics and climate feedbacks. Nature 451, 289–292.
Hopkins, F.M., Torn, M.S., Trumbore, S.E., 2012. Warming accelerates decomposition of decades-old carbon in forest soils. Proc. Natl. Acad. Sci. U. S. A. 109, 1753–1761.
Karhu, K., Fritze, H., Tuomi, M., Vanhala, P., Spetz, P., Kitunen, V., Liski, J., 2010. Temperature sensitivity of organic matter decomposition in two boreal forest soil profiles. Soil Biol. Biochem. 42, 72–82.
Knorr, W., Prentice, I.C., House, J.I., Holland, E.A., 2005. Long-term sensitivity of soil carbon turnover to warming. Nature 433, 298–301.
Kuzyakov, Y., 2010. Priming effects: Interactions between living and dead organic matter. Soil Biol. Biochem. 42, 1363–1371.
Larionova, A.A., Yevdokimov, I.V., Bykhovets, S.S., 2007. Temperature response of soil respiration is dependent on concentration of readily decomposable C. Biogeosciences 4, 1073–1081.
Li, J.W., Ziegler, S., Lane, C.S., Billings, S.A., 2012. Warming-enhanced preferential microbial mineralization of humified boreal forest soil organic matter: Interpretation of soil profiles along a climate transect using laboratory incubations. J. Geophys. Res. Biogeosci. 117, G02008.
Lin, Q., Brookes, P.C., 1999. An evaluation of the substrate-induced respiration method. Soil Biol. Biochem. 31, 1969–1983.
Luo, Y.Q., Zhou, X.H., 2006. Soil Respiration and the Environment. Academic Press, Elsevier.
Macdonald, N.W., Zak, D.R., Pregitzer, K.S., 1995. Temperature effects on kinetics of microbial respiration and net nitrogen and sulfur mineralization. Soil Sci. Soc. Am. J. 59, 233–240.
Olk, D.C., 2006. A chemical fractionation for structure-function relations of soil organic matter in nutrient cycling. Soil Sci. Soc. Am. J. 70, 1013–1022.
Parton, W.J., Schimel, D.S., Cole, C.V., Ojima, D.S., 1987. Analysis of factors controllings soil organic-matter levels in great-plains grasslands. Soil Sci. Soc. Am. J. 51, 1173–1179.
Paustian, K., Parton, W.J., Persson, J., 1992. Modeling soil organic-matter in organic-amended and nitrogen-fertilized long-term plots. Soil Sci. Soc. Am. J. 56, 476–488.
Pendall, E., King, J.Y., 2007. Soil organic matter dynamics in grassland soils under elevated CO_2: insights from long-term incubations and stable isotopes. Soil Biol. Biochem. 39, 2628–2639.
Plante, A.F., Conant, R.T., Carlson, J., Greenwood, R., Shulman, J.M., Haddix, M.L., Paul, E.A., 2010. Decomposition temperature sensitivity of isolated soil organic matter fractions. Soil Biol. Biochem. 42, 1991–1996.
Raich, J.W., Potter, C.S., 1995. Global patterns of carbon-dioxide emissions from soils. Glob. Biogeochem. Cycles 9, 23–36.
Rasmussen, C., Southard, R.J., Horwath, W.R., 2006. Mineral control of organic carbon mineralization in a range of temperate conifer forest soils. Glob. Change Biol. 12, 834–847.
Rey, A., Jarvis, P., 2006. Modelling the effect of temperature on carbon mineralization rates across a network of European forest sites (FORCAST). Glob. Change Biol. 12, 1894–1908.
Rey, A., Pegoraro, E., Jarvis, P.G., 2008. Carbon mineralization rates at different soil depths across a network of European forest sites (FORCAST). Eur. J. Soil Sci. 59, 1049–1062.
Schimel, J.P., Weintraub, M.N., 2003. The implications of exoenzyme activity on microbial carbon and nitrogen limitation in soil: a theoretical model. Soil Biol. Biochem. 35, 549–563.
Schmidt, M.W.I., Torn, M.S., Abiven, S., Dittmar, T., Guggenberger, G., Janssens, I.A., Kleber, M., Kogel-Knabner, I., Lehmann, J., Manning, D.A.C., Nannipieri, P., Rasse, D.P., Weiner, S., Trumbore, S.E., 2011. Persistence of soil organic matter as an ecosystem property. Nature 478, 49–56.
Six, J., Conant, R.T., Paul, E.A., Paustian, K., 2002. Stabilization mechanisms of soil organic matter: Implications for C-saturation of soils. Plant Soil 241, 155–176.
Sollins, P., Homann, P., Caldwell, B.A., 1996. Stabilization and destabilization of soil organic matter: mechanisms and controls. Geoderma 74, 65–105.
Stres, B., Danevcic, T., Pal, L., Fuka, M.M., Resman, L., Leskovec, S., Hacin, J., Stopar, D., Mahne, I., Mandic-Mulec, I., 2008. Influence of temperature and soil water content on bacterial, archaeal and denitrifying microbial communities in drained fen grassland soil microcosms. Fems Microbiol. Ecol. 66, 110–122.
Traore, S., Thiombiano, L., Millogo, J.R., Guinko, S., 2007. Carbon and nitrogen enhancement in Cambisols and Vertisols by *Acacia* spp. in eastern Burkina Faso: Relation to soil respiration and microbial biomass. Appl. Soil Ecol. 35, 660–669.
van Hees, P.A.W., Johansson, E., Jones, D.L., 2008. Dynamics of simple carbon compounds in two forest soils as revealed by soil solution concentrations and biodegradation kinetics. Plant Soil 310, 11–23.
Verberne, E.L.J., Hassink, J., de Willigen, P., Groot, J.J.R., van Veen, J.A., 1990. Modeling organic-matter dynamics in different soils. Neth. J. Agric. Sci. 38, 221–238.
von Lutzow, M., Kogel-Knabner, I., 2009. Temperature sensitivity of soil organic matter decomposition-what do we know? Biol. Fertil. Soils 46, 1–15.
von Lutzow, M., Kogel-Knabner, I., Ekschmitt, K., Matzner, E., Guggenberger, G., Marschner, B., Flessa, H., 2006. Stabilization of organic matter in temperate soils: mechanisms and their relevance under different soil conditions – a review. Eur. J. Soil Sci. 57, 426–445.
von Lutzow, M., Kogel-Knabner, I., Ekschmittb, K., Flessa, H., Guggenberger, G., Matzner, E., Marschner, B., 2007. SOM fractionation methods: relevance to functional pools and to stabilization mechanisms. Soil Biol. Biochem. 39, 2183–2207.
Waldrop, M.P., Firestone, M.K., 2004. Altered utilization patterns of young and old soil C by microorganisms caused by temperature shifts and N additions. Biogeochemistry 67, 235–248.
Wang, W.J., Baldocka, J.A., Dalala, R.C., Moody, P.W., 2004. Decomposition dynamics of plant materials in relation to nitrogen availability and biochemistry determined by NMR and wet-chemical analysis. Soil Biol. Biochem. 36, 2045–2058.

Wang, W.J., Dalal, R.C., Moody, P.W., Smith, C.J., 2003. Relationships of soil respiration to microbial biomass, substrate availability and clay content. Soil Biol. Biochem. 35, 273–284.
West, A.W., Sparling, G.P., 1986. Modifications to the substrate-induced respiration method to permit measurement of microbial biomass in soils of differing water contents. J. Microbiol. Methods 5, 177–189.
Xu, X., Zhou, Y., Ruan, H.H., Luo, Y.Q., Wang, J.S., 2010. Temperature sensitivity increases with soil organic carbon recalcitrance along an elevational gradient in the Wuyi Mountains, China. Soil Biol. Biochem. 42, 1811–1815.
Zogg, G.P., Zak, D.R., Ringelberg, D.B., MacDonald, N.W., Pregitzer, K.S., White, D.C., 1997. Compositional and functional shifts in microbial communities due to soil warming. Soil Sci. Soc. Am. J. 61, 475–481.